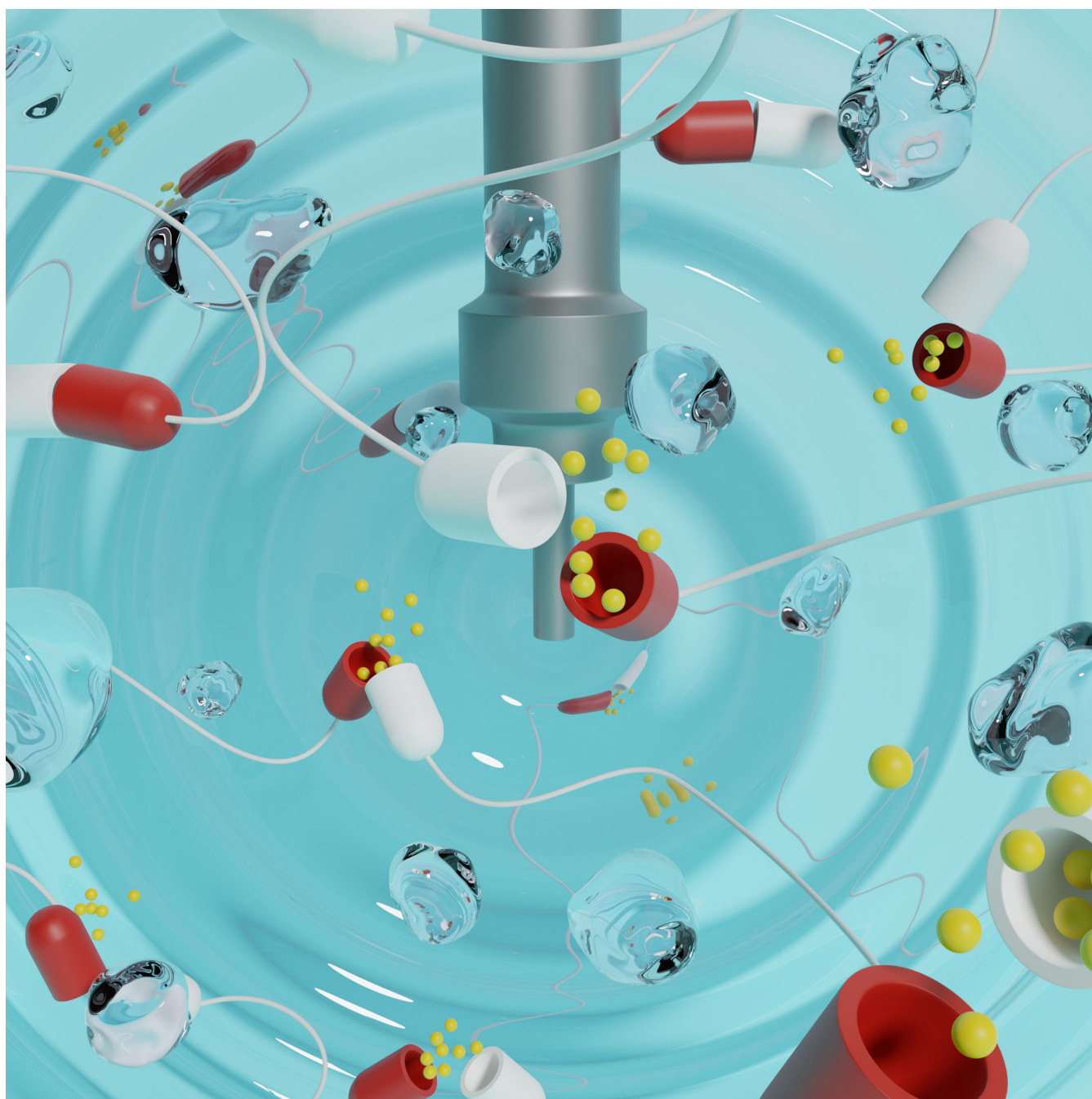


🏆 Release of Molecular Cargo from Polymer Systems by Mechanochemistry

Robin Küng,^[a] Robert Göstl,^[b] and Bernd M. Schmidt*^[a]



Abstract: The design and manipulation of (multi)functional materials at the nanoscale holds the promise of fuelling tomorrow's major technological advances. In the realm of macromolecular nanosystems, the incorporation of force-responsive groups, so called mechanophores, has resulted in unprecedented access to responsive behaviours and enabled sophisticated functions of the resulting structures and advanced materials. Among the diverse force-activated motifs, the on-demand release or activation of compounds,

such as catalysts, drugs, or monomers for self-healing, are sought-after since they enable triggering pristine small molecule function from macromolecular frameworks. Here, we highlight examples of molecular cargo release systems from polymer-based architectures in solution by means of sonochemical activation by ultrasound (ultrasound-induced mechanochemistry). Important design concepts of these advanced materials are discussed, as well as their syntheses and applications.

1. Introduction


The ability to precisely manipulate the smallest particles and to control the structure and function of nano- and macromolecular systems using external stimuli has emerged as a promising strategy for producing reconfigurable or multifunctional devices and programmable nanomaterials.^[1,2] A variety of responsive systems have been reported using light, pH, temperature, magnetic fields, and chemical stimuli as triggers, playing important roles in many applications in different disciplines, including nanotechnology, biochemistry, medicine, materials science, polymer science, and engineering.^[1] Light, with its high spatiotemporal and energetic resolution, has established itself as the most common precision stimulus that, in combination with embedded photoswitches, allows the reversible control of complex systems.^[3] However, light also suffers from disadvantages, such as low penetration depths into materials and tissues as well as occasional phototoxicity. In contrast, mechanical force is a ubiquitous stimulus that carries the stigma of a destructive disposition. Yet, exciting productive transformations that would be otherwise impossible have been implemented by chemistry under mechanical force: mechanochemistry.^[4] Because of the all-embracing general term mechanochemistry that encompasses all chemical transformations caused by the action of force on matter, contemporary mechanochemistry is broad and diverse.^[2a] It is manifested in four principal subfields: tribochemistry, trituration, sonochemistry, and polymer mechanochemistry.^[2,5] Here we will mostly cover aspects of polymer mechanochemistry induced by ultrasound and compression.


The force required to induce a mechanochemical reaction can be in principle exerted on a bulk material by macroscopic deformation by grinding, ball-milling, compression or extension, and shearing. Alternatively, forces can be transduced to chemical bonds by sonication in solution or at the molecular scale by using, for example, atomic force microscopy.^[2d] Mechanophores are force-sensitive molecular units with mechanically labile bonds that, when incorporated within polymers, undergo chemical transformations at a higher rate than other components of the polymer when mechanically stressed.^[2n] Since it is not possible to cover all areas where mechanophores are applied, we selected publications which we deemed interesting to the general reader and which, according to our perception, were highly relevant and timely in respect to our focus on release processes. Excellent review articles cover other aspects of this exciting field. For example, force-sensitive functional units with latent optical properties (optical force probes) can be designed and incorporated into polymer materials to visualize force-induced events, with the goal of producing materials with macroscopically observable visual output, allowing for quick assessment.^[2e,r,s] Alongside, several reviews on force-responsive materials,^[2a,d,k,o] pericyclic reactions,^[2f] interlocked structures,^[2h] and mechanocatalysis^[2n] are available for the interested reader, which offer interesting and detailed insights into the respective fields.

It is important to keep in mind that the force experienced by the mechanophore at the molecular level depends on the nature of the exerted macroscopic force. In all cases, the influence of mechanical force on molecular reactivity relies on the coupling of forces to specific bonds. In polymer mechanochemistry, polymer chains are used for this purpose.^[2n] For example, the tension generated by extensional shear flow induces force accumulation at the centre of the polymer chain, whereas static tension distributes force evenly along the polymer. The consequences of an uneven force distribution in extensional shear lead to a preference for midchain scission in polymers during exposure to pulsed ultrasound.^[2o] Typical laboratory immersion probe sonicators used for mechanochemistry operate at frequencies around 20 kHz. Power intensities can be high, above $10 \text{ W} \cdot \text{cm}^{-2}$ and generally lead to inertial cavitation in liquid media. Such high intensities can induce chemical changes or produce significant effects by direct sonochemical action.^[2j] The growth and subsequent collapse of cavitation bubbles in solution create a substantial velocity

[a] R. Küng, Dr. B. M. Schmidt
Institut für Organische Chemie und Makromolekulare Chemie
Heinrich-Heine-Universität Düsseldorf
Universitätsstraße 1, 40225 Düsseldorf (Germany)
E-mail: Bernd.Schmidt@hhu.de

[b] Dr. R. Göstl
DWI – Leibniz Institute for Interactive Materials
Forckenbeckstr. 50, 52056 Aachen (Germany)

 Selected by the Editorial Office for our Showcase of outstanding Review-type articles <http://www.chemeurj.org/showcase>.

 © 2021 The Authors. Chemistry - A European Journal published by Wiley-VCH GmbH. This is an open access article under the terms of the Creative Commons Attribution Non-Commercial License, which permits use, distribution and reproduction in any medium, provided the original work is properly cited and is not used for commercial purposes.

gradient along the polymer backbone, leading to non-equivalent force contributions at different polymer chain segments, with the strain rate having a clear time dependence on the radius of the imploding bubble.^[2m] Forces near the centre of the polymer chain are sufficient to induce bond scission in mechanophores after they (partially) stretch and unravel the coiled polymer (Figure 1). This differential force distribution is further supported by a lack of mechanophore activation when the mechanophore is placed at the end of polymer chains.^[2m,o]

In principle, two types of bond scission are observed during sonication. The productive breaking of the mechanophore itself is described as specific bond scission. Random chain cleavage, also known as non-specific bond scission, occurs in all polymers during sonication and generally is a competitive, undesired side reaction as it is mostly unproductive. As a result, selectivity in

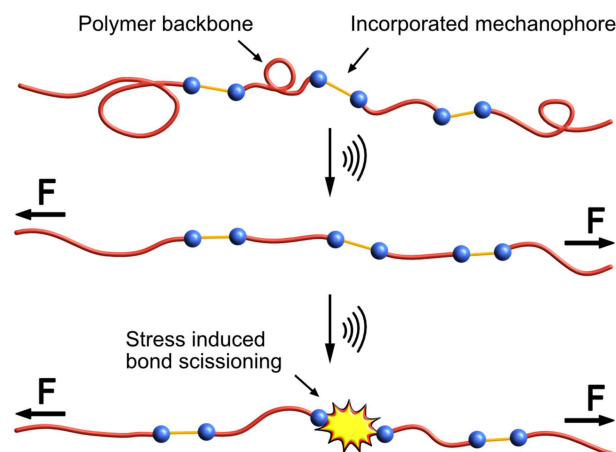


Figure 1. Force-induced bond scission occurs at the incorporated mechanophore (orange and blue) in a polymer backbone (red). Depending on the functional groups and the surrounding environment, different levels of energy are needed for stretching or structural distortion of the polymer backbone to overcome attractive intermolecular interactions, depicted by the unwinding of the polymer coil.^[2]

Robin Küng received his B.Sc. and M.Sc. in chemistry from the Heinrich Heine University, Düsseldorf in 2016 and 2018, respectively. Robin is currently a Ph.D. student in the group of Bernd and was awarded a Manchoth Fellowship of the Jürgen Manchoth Fund in 2019. His research focuses on the sonochemical activation of polymer-embedded, metal-organic supramolecular cages for cargo release.



Robert Göstl studied chemistry at the Humboldt-Universität zu Berlin. There, he obtained his diploma degree in 2011 and his doctoral degree in 2014, working on photoswitchable diarylethenes. In his postdoctoral research, he started working on polymer mechanochemistry at Eindhoven University of Technology until 2016. He is currently leading an independent research group at DWI that develops molecular tools to understand and harness mechanical force in polymer materials.



Bernd M. Schmidt investigates responsive and functional supramolecular systems. Born and raised in Berlin, Germany, he did his Ph.D. with Dieter Lentz at the Freie Universität Berlin and with Hidehiro Sakurai at the IMS in Okazaki, Japan, working on bowl-shaped aromatic hydrocarbons. Bernd stayed with a Humboldt research fellowship with Makoto Fujita at the University of Tokyo, Japan, and with Stefan Hecht at the HU Berlin, Germany. Since February 2018, he has been an independent research group leader at the HHU Düsseldorf in Germany, where he became a Member of the Young Academy of the North Rhine-Westphalian Academy of Sciences, Humanities and the Arts in 2020.



terms of the identity of the cleaved bond can only be achieved by tailoring the mechanophore to exhibit a higher force-dependent scission rate than the polymer backbone or other functional moieties.^[6] It is also possible that chains are cleaved multiple times during a single cavitation event, if the fragments produced have sufficient contour length at the present strain rate.^[2m] Forces necessary for bond rupture depend on the nature of the bonds, in addition to the energy requirement for stretching or structural distortion of the polymer backbone, also overcoming present intermolecular interactions depending on the functional groups and the surrounding environment. Famously weak covalent bonds such as the peroxide O–O bond have a thermal bond dissociation energy (BDE) of around 35 kcal mol⁻¹, disulfide bonds (BDE ca. 60 kcal mol⁻¹), with coordinate covalent bonds ranging from 36 kcal mol⁻¹ for palladium-phosphorus to 61 kcal mol⁻¹ for silver-carbene coordinative bonds, and BDE ca. 66 kcal mol⁻¹ for ruthenium-carbene coordinative bond, which all will be discussed explicitly in the following. Bonds have been labelled as strong bonds from a mechanochemical point of view with thermal BDEs exceeding 72 kcal mol⁻¹ (C–C and C–N bonds).^[2] Bond lengths are another important parameter that can be altered by molecular design to tune the force-reactivity.^[7]

2. Mechanoacid Generators

The proton is one of the simplest and most used chemical species and has a wide variety of applications in polymer chemistry, including phase transition,^[8] controlled polymer degradation,^[9] cross-linking,^[10] and ring opening polymerization.^[11] The group of Moore synthesised a cross-linked polymer containing mechanophore 1 based on a *gem*-dichlorocyclopropane (gDCC) motif, which undergoes a mecha-

nochemical rearrangement to 2-chloronaphthalene (**2**), while formally releasing HCl (Figure 2, a).

The release was triggered by compressing the mechanophore in a pellet press (880 to 3520 bar pressure), which resulted in approximately 20% activation of the mechanophore as measured by differential scanning calorimetry (DSC) and a molecular change was confirmed by confocal Raman spectroscopy (appearance of aromatic C=C stretch peaks). The mechanophore activation also correlated with compressive loading. To further validate the true release of HCl, Methyl red, a pH indicator that is orange in MeCN and pink when exposed to acids, was employed. A noticeable colour change was observed when a compressed sample of mechanophore **1** was submerged in the indicator solution.^[12] While the latter system lacked thermal stability, a next generation of mechanogenerated acids addressed this by establishing symmetrical oxime sulfonate groups as a thermally stable mechanophore **3** (Figure 2, b). Ultrasonication of **3** resulted in a decrease in molar mass of approximately 50% ($M_n = 103.2$ kDa) of the original polymer ($M_n = 189.4$ kDa) after 30 min. Successful activation was further verified by ¹⁹F NMR, which showed that the bond scission occurred at the mechanophore or in close proximity to it. Upon sonication, the pH value was measured in MeCN/H₂O. The addition of H₂O is necessary to induce acid formation from generated sulfonyloxyl (RSO₃[•]) or sulfonyl (RSO₂[•]) radicals. A steady decrease in the pH could be observed with increasing sonication time, confirming the liberation of protons in solution.^[13] The acid generation of mechanophore **3** is directly coupled to bond scission, limiting the generation to one proton per bond breakage. Craig and co-workers were able to overcome this issue by utilizing alkoxy-derivatized gDCCs (Figure 2, c). These show a unique behaviour by releasing HCl when being thermally activated.^[14] This modified gDCC was incorporated

into a multimechanophore architecture with a proportion of 47 mol% of MeO-gDCC by incorporating multiple repeat units to yield the final polymer **5**.^[15] After esterifying to give the terminal dienes with 4-pentenoic anhydride, ring-closing metathesis (RCM) yielded a macrocycle that was reacted again using ring-opening metathesis polymerization (ROMP). During sonication, a decrease of the M_n to 26 kDa was observed and three new species (**6a**, **6b**, and **6c**) were identified by ¹H NMR. Rhodamine B, a pH indicator, was added to the sonicated solution to confirm the release of HCl. An activation of MeO-gDCC of approximately 65% was achieved, which corresponds to about 0.58 equiv. of HCl per activated bond. UV/Vis spectroscopy was used to monitor the formation of HCl during sonication over the course of 4 h, and an increase in the characteristic absorption spectrum of protonated rhodamine B was observed. In a demonstration for potential applications, the mechanoacid **5** and pH indicator rhodamine B were covalently embedded into a poly(dimethylsiloxane) (PDMS) network. When tensile strain was applied to a film thereof, HCl was released, activating the pH indicator, with the concomitant colour change occurring at the deformed area of the polymer. Due to the bimolecular reaction (release and protonation) of this mechanophore, the colour change was not instantaneous but evolved over several minutes. The fluorescence of protonated rhodamine can also be observed under 365 nm irradiation. Further, a PDMS cylinder was exposed to global and local compression, where fluorescence and mechanochromic response could be observed.^[15] While various types of photoacids^[16] and mechanochromically responsive systems are already well known,^[17] these works are of considerable interest for potential applications such as self-healing, self-reinforcing, or other, advanced force-responsive systems.

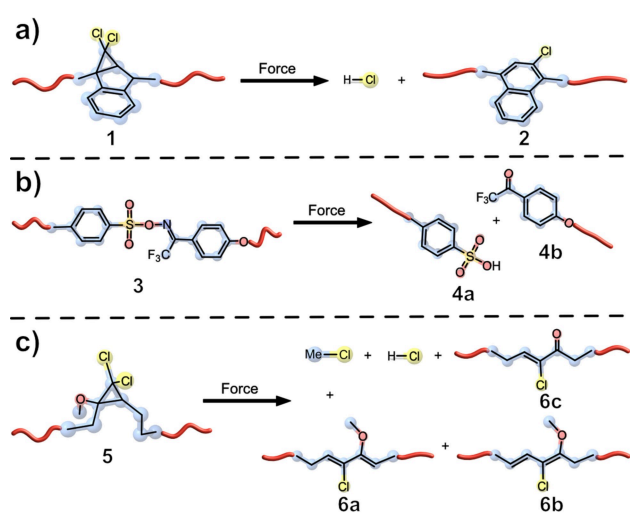


Figure 2. Different approaches for force-induced acid generation. a) gDCC from indene (**1**) rearranged to 2-chloronaphthalene (**2**), while formally releasing HCl;^[12] b) oxime sulfonate mechanophores produce trifluoromethyl ketone moieties and an acid, which is thought to be an aryl sulfonic acid;^[13] c) alkoxy substituted MeO-gDCCs released either HCl or MeCl, with 0.58 equiv. of HCl released per mechanophore activation and 67 protons released per chain scission event.^[15]

3. Molecular Release Systems

Boydston and colleagues investigated the release of small molecules from polymeric scaffolds while keeping the polymer's overall structure intact.^[18,19] They designed a sophisticated, oxanorbornadiene-based mechanophore **7** that, upon compression in the bulk, releases benzyl furfuryl ether via a retro [4 + 2] cycloaddition reaction (Figure 3, a).

The authors hypothesized that the conversion of the alkene to an alkyne should, in principle, result in a strengthened polymer backbone.^[18] This force-guided linearization (coined flex activation) of the ene-diester **7** required an activation energy of 35 kcal mol⁻¹ as suggested by constrained geometry simulated external force (CoGEF) computations.^[20] The synthesised poly(methyl acrylate) (PMA) network was cross-linked with mechanophore **6** in different quantities (5 and 14 mol%). For the mechanochemical activation, each network was compressed for 30 min in a carver press at various pressures (0 to 12000 bar) with a maximum activation of 9.5% observed at 12000 bar. The samples were washed with CH₂Cl₂ and the released benzyl furfuryl ether was detected by GC-MS. In addition, confocal Raman spectroscopy of the network displayed a new band at 2250 cm⁻¹ which was attributed to the

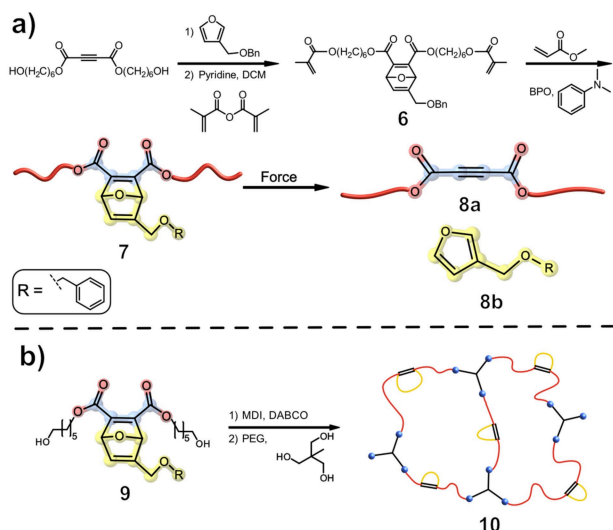


Figure 3. Oxanorbomadiene-based mechanophore **7** embedded in a network formed by polymerization with methyl acrylate. a) Mechanophore activation led to a cycloelimination of the [4 + 2] adduct, ultimately releasing the benzyl furfuryl ether **8b**.^[18] b) PMA was exchanged for a polyurethane (PU) network **10** to reduce macroscopic failure.^[22]

stretching frequencies of acetylenedicarboxylate. For both cross-linked networks, a monotonic rise with increasing pressure could be observed for the mechanochemical activation. A greater release of furan **8b** was observed for the cross-linked network having a higher amount of mechanophore **6**, supporting a nonthermal mechanism during compression. Furthermore, the cross-linked network **7** was compressed at 6000 bar for different lengths of time (1 and 30 min), resulting in an activation of approximately 3% in both cases, which is in accordance with the activation mechanism.^[18,21] As a result, Boydston and colleagues elegantly demonstrated that a small molecule, which is not part of the elongated polymer chain can be released.

The proposed design was clever, but suffered from the limited activation achieved after only one compression event before the required force caused the sample to fail macroscopically.^[18] Boydston and co-workers were able to overcome this problem by using an elastomer matrix. This polymeric scaffold was anticipated to be able to recover from the initial mechanochemical activation and, therefore, could undergo multiple compression and activation cycles. To achieve these elastomeric properties, the previous used PMA was exchanged for a polyurethane (PU) network containing flexible polyether segments and hard diol-diisocyanate chain extenders, resulting in enhanced elasticity and strength (Figure 3, b).^[22,23]

The mechanochemical activation was tested by exposing the polymer **10** for one minute to sustained pressure (0 to 3500 bar) in a hydraulic press. GC-MS was used to quantify the release of benzyl furfuryl ether, and a continuous increase in activation was observed, reaching a maximum of 6% activation for the cross-linked polymer with mechanophore **10**.^[22] In contrast to the previous reported PMA-network, only 1760 bar were necessary to achieve 6% activation.^[18] To ultimately prove

that multiple compression- and activation cycles are feasible for mechanophore **10**, two samples were compressed at 350 and 880 bar for 1 min. After compression, the sample was folded and compressed again for 1 min. The method was repeated for each sample, until the desired number of compressions was reached. Again, the compressed samples were washed with CH_2Cl_2 and the released furan **8b** was detected by GC-MS, proving an iterative increase in the activation of mechanophore **10**. While the compression with 880 bar showed a greater activation of the mechanophore **10** at first, both samples achieved their maximum activation of 6–7% after approximately nine consecutive compressions. Boydston and co-workers reasoned that the polymer had softened to the point where additional activation could not be achieved by applying more tensile strength.^[22] It was assumed that a strain softening effect of the polymer occurred with each compression. This is often attributed to force-induced bond breakage in hard domains of the polymer.^[23] To investigate this behaviour, the group compressed the same samples several times before measuring the flexural modulus. Unlike the previous experiment, the rectangular samples were larger and were not folded after each compression. It was possible to show that the material softens faster with higher tensile force (880 bar). After only one compression, the sample's flexural modulus was reduced to 68% of its initial value. In comparison, the sample compressed at 350 bar retained 86% of its flexural modulus for up to nine compressions. This behaviour was explained with random bond scission across the cross-linker or the destruction of the network's hard domains.^[22,24] The group was able to demonstrate, in both cases, the flex activation of their mechanophore, following the release of pre-installed small molecules and bond strengthening of the polymeric backbone. By modifying the polymeric network, the problem of macroscopical failure could be overcome and multiple activation cycles were possible.

In a recent study, Boydston and co-workers were capable of demonstrating the flex-activation of a mechanophore **11a** which is based on N-heterocyclic carbene-carbodiimide (NHC-CDI) adducts, which are of great interest due to their diverse applications, from organometallic chemistry to organocatalysis.^[25,26] Free 1,3-bis(2,6-diisopropylphenyl)imidazolylidene was used to generate mechanophore **11a**, which was incorporated as a cross-linker into a PMA network (Figure 4).

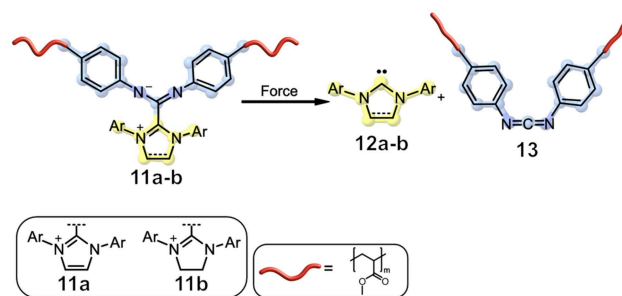


Figure 4. Carbene release **12a–b** from an N-heterocyclic carbene-carbodiimide adduct in a PMA network **11a–b**.^[26]

Phenyl isothiocyanate (PITC) was then employed as a trapping agent for the released NHC **12a** in the following compression tests and the resulting NHC-PITC adduct was quantified by LC-MS. During compression, an activation of 0.41% could be achieved at 7400 bar. With an increasing number of compressions, a monotonic rise in activation could again be observed, up to a maximum of 1.06%. This increase in activation is in contrast to previously reported PMA network compression, which failed macroscopically due to strain softening. The addition of liquid PITC to the PMA network was thought to plasticize the polymer and thus improve its durability. To demonstrate the adaptability of employed NHCs, NHC-CDIs based on 1,3-bis(2,6-diisopropylphenyl)imidazolidin-2-ylidene (SIPr) were incorporated into the PMA network **11b** and 0.4% of the mechanophore was activated after compression at 7400 bar for 10 minutes.^[26] The approach of flex activation was also used by the group of Kilian and co-workers, who incorporated oxanorbornadiene **6** into a double network hydrogel consisting of two interpenetrated networks. A flexible network with reversible bonds supports one brittle network that contains the mechanophore. When this combined network is stressed, the mechanophore in the densely crosslinked network breaks and releases furfuryl **8b**, whereas the flexible network keeps the material intact. Compression tests showed that a cargo release of 20% at 10 bar could be achieved. The force needed for this activation is significantly lower in contrast to the previous reported results and was attributed to the aqueous environment as well as the elastic interpenetrated networks.^[27]

In recent years, a variety of mechanophores capable of visualizing stress or damage in polymeric scaffolds have been developed.^[28] Especially noteworthy mechanophore used for this application are spiropyrans (SP) implemented by Sottos group and Moore group.^[29–31] Craig and co-workers further investigated if a stress responsive molecule could be incorporated into a PDMS network to release small molecule cargo. Based on the previously discussed “flex activation”^[(18,22)] a phenyltriazolinedione-anthracene adduct^[32] **14** was chosen as the mechanophore and embedded into PDMS. Mechanochemical activation led to a force-induced planarization of the fluorescent anthracene **16** while simultaneously releasing phenyltriazolinedione **15** in a retro-Diels-Alder reaction (Figure 5).

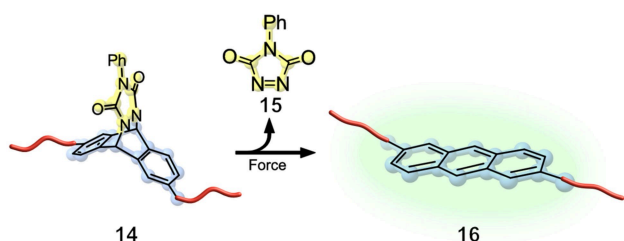


Figure 5. In a PDMS network (red), the Diels-Alder adduct of anthracene and phenyltriazolinedione was used as a cross-linker. Tension accelerated the flex-activated retro Diels-Alder reaction, resulting in dienophile release accompanied by turn-on of the anthracene fluorescence.^[33]

Since these adducts were less reactive than anticipated, elevated temperatures were needed for the mechanochemical activation. The reactivity was compared depending on the temperature necessary to evaluate the release. Therefore, two films, one kept unstrained and one kept under 175% strain, were exposed to increasing heat. Under strain tension, an activation of approximately 1% at 125 °C could be observed spectroscopically, with increasing activation at higher temperatures. After relaxation and cooling, the anthracene mechanophore system **16** underwent shape recovery as described for the SP-mechanophore.^[33] Otsuka's group reported the release of the small fluorescent molecule, fluorenone **18**, using a novel organic peroxide mechanophore **17**. Therefore, a bis(9-methylphenyl-9-fluorenyl) peroxide unit was incorporated into different polymeric networks. Upon mechanochemical activation, bond scission occurred at the peroxide moiety, which dissociates into highly reactive oxygen-centred radicals. These radicals can further undergo β -scission, resulting in a carbon-centred radical and fluorenone **18**. Otsuka and co-workers were able to perform the mechanochemical release of 9-fluorenone via grinding and compression, allowing for potential application when designing stress-responsive materials (Figure 6).^[34]

Robb's group introduced another mechanophore platform for small molecule cargo release, based on the concept of mechanical gating, in which a mechanophore initially prevents the reaction of another “masked” functionality.^[35–38] The introduced furan-maleimide Diels-Alder adduct **19a–b** was sonicated to initiate a cascade reaction, which resulted in a retro Diels-Alder reaction that revealed maleimide **20** and a metastable furfuryl carbonate **21a–b**. This carbonate decomposes in polar protic media, releasing carbon dioxide and coumarin as the cargo load (Figure 7).

The substitution of the furfuryl-adduct plays a vital role for cargo release. An unsubstituted furfuryl model compound based on **21a** had a decomposition time half-life in MeCN/MeOH of several weeks, whereas substitution with an α -methyl group (intermediate **21b**) decreased the half-life significantly to $t_{1/2} = 79$ min. For the mechanochemical activation, the polymer **21b** was sonicated (1 s on/2 s off, 20 kHz, $8.2 \text{ W} \cdot \text{cm}^{-2}$) for approximately 3 h. The release of the photoluminescent coumarin **22a** was monitored by fluorescence spectroscopy and the decrease in molar mass was measured by GPC. A steady

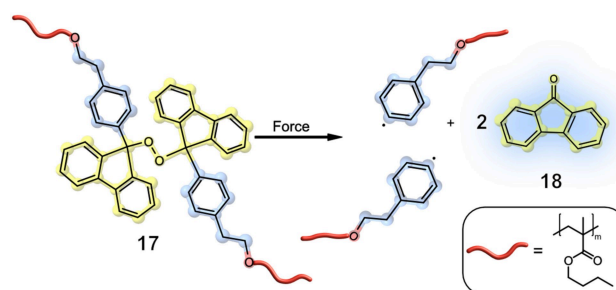


Figure 6. Organic peroxide mechanophores can be incorporated into a polymer network to release fluorescent **18** and have potential for application in designing stress-responsive materials.^[34]

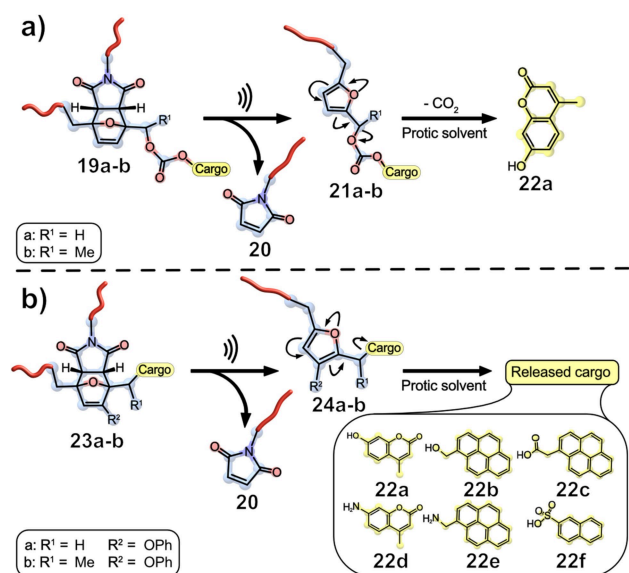


Figure 7. Furan-maleimide Diels-Alder adducts are potent mechanophores for cargo release. a) Fluorogenic coumarin was released after a cascade reaction, allowing for tracking of the reaction progress by using fluorescence spectroscopy in addition to commonly employed NMR spectroscopy.^[36] b) A wide range of cargo scope, such as alcohol, alkylamine, arylamine, carboxylic acid, and sulfonic acid.^[37]

decrease in M_n could be observed during sonication over a period of 150 min, whereupon a successful release of 64% of hydroxycoumarin **22a** was detected. A maximum release value of 87% was calculated by fitting the data to a first-order rate expression. The reduced efficiency was attributed to non-specific bond scission during sonication.^[36] The promising concept of a gated mechanophore platform makes it possible to independently control and tune the properties of the mechanophore and the masked derivative.

Mechanophore **19** is an excellent example of a gated mechanical system, but it lacks the ability to release a diverse range of cargo since it is limited to phenolic compounds and due to its relatively slow decomposition time of approximately 1 h. As an example, the substitution of hydroxycoumarin through a primary alcohol would already increase the half-time of the release to 4 d, making mechanophore **19** impracticable for applications. DFT calculations of different substitution patterns suggested that a combination of an α -methyl group and an electron donating phenoxy group at the 3-position of the furan ring would decrease the activation energy for the decomposition significantly. Whereas the previous model mechanophore based on **19b** had an activation energy of 22.0 kcal·mol⁻¹, the optimized substitution pattern for the mechanophore would lead to a decrease to 18.3 kcal·mol⁻¹ for carbonate compounds and to 23.8 kcal·mol⁻¹ for the carbamates. These calculations suggested even the release of amine-derived compounds would be achieved on a reasonable time scale. The effect of substitution was tested with different hydroxy- and aminocoumarin compounds, as seen in Figure 8.

Cargo release was monitored using photoluminescence spectroscopy for coumarin. As expected, the decomposition of

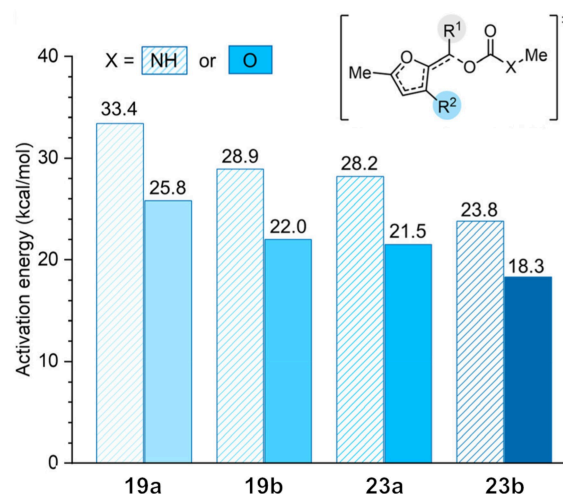


Figure 8. Substituent effects on the reactivity of 2-furancarbinol derivatives. Corresponding activation energies for fragmentation of the α -C–O bond calculated at the M06-2X/6-311 + G** level of density functional theory.^[37] Reproduced from Ref. [37] with permission. Copyright 2021, American Chemical Society.

carbonate mechanophores is faster than that of the corresponding carbamates, and a higher substitution pattern led to a faster release for both cargo types. It is worth noting that the release of hydroxycoumarin was instantaneous for carbonates **23a** and **b**. For the carbamates, the half-life time from **19b** could be decreased from 240 d to 41 min (**23b**). To demonstrate the broad molecular scope of feasible cargo molecules, the group incorporated further functional groups depicted in Figure 7, b. The triggered cargo release for these mechanophores was achieved in reasonable time. Robb and co-workers implemented a new gated mechanical system which, upon sonication, is capable of releasing diverse cargo with high yields and fast rates.^[37,38]

The groups of Herrmann and Göstl reported the release of furan containing small-molecule drugs through sonochemical activation. Therefore, they utilized polymers with mechanochemically latent central disulfide bonds. Upon ultrasonication, bond scission occurs at the S–S moiety, generating thiyl radicals followed by protonation by H₂O, ultimately leading to a thiol functionality. In a cascade-like reaction, the thiol **26** undergoes a Michael-type addition with oxanorbornadiene **27** to finally release the small molecule drug **28a–c** in a retro Diels-Alder reaction (Figure 9, a).^[39] In a proof-of-concept experiment, the researchers used thiol **29** in the presence of DIPEA to produce furan-dansyl **28a** (Figure 9, b), which was analysed using ¹H NMR, UV/Vis, and fluorescence spectroscopy. An excess of PEG-SH in relation to the oxanorbornadiene adduct **28a** had to be used to achieve a cargo release of 95% after 72 h. In situ and ex situ studies confirmed the mechanochemical release of furan-dansyl **28a** during ultrasonication.

With these results, the mechanochemical activation of pharmacologically relevant drugs, like intrinsically furan-bearing furosemide and furylated doxorubicin (DOX), was investigated. Sonication of the disulfide-centred polymer **25** was conducted

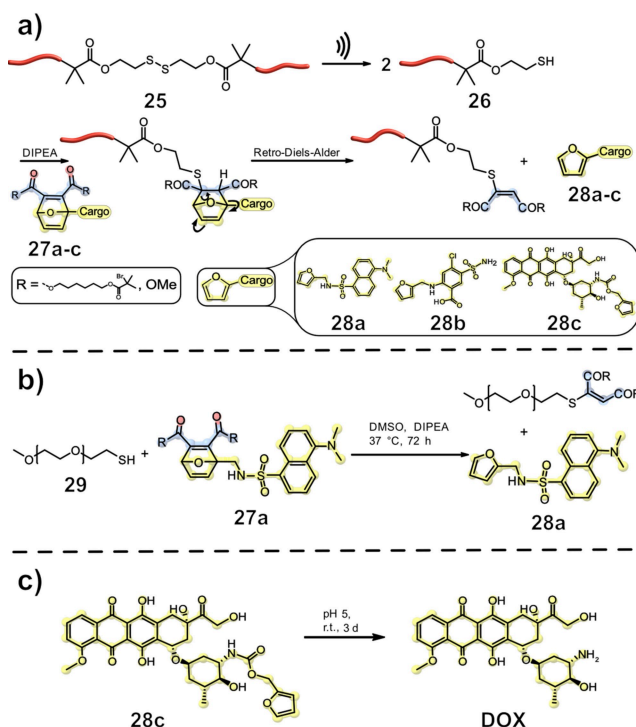


Figure 9. The force-induced intermolecular release of drugs using disulfide mechanophores. First, the disulfide was cleaved and protonated, after which the resulting thiol underwent Michael-addition to the oxanorbornene structure, upon which elimination of the furan-bearing drug proceeded.^[39]

in the presence of the furosemide adduct **27a** and DIPEA for 75 min. Subsequent analysis revealed the release of **28a** by ¹H NMR and UPLC-MS. The furan-bearing drug **28a** is a diuretic medication used in the treatment of chronic cardiovascular, pulmonary, and kidney diseases.^[40] High dose therapy with the medicament can lead to diuresis, ultimately resulting in dehydration, hypotension, or vascular clot formation.^[41] Therefore, control over the release of furosemide **28a** is desirable.

Whereas the previous released example was a furan-containing drug, the groups of Herrmann and Göstl considered if the scope could be further expanded to overcome the dependency on the intrinsic furan functionality. Doxorubicin **DOX**, which was chosen for this application, is one of the most used antitumor anthracycline antibiotics in the treatment of a variety of cancers.^[42] Its short half-life and high toxicity make controlled release desirable. Upon ultrasonication of disulfide-centred polymer **25** for 90 min and subsequent addition of Diels-Alder adduct **28c** and DIPEA, the release of **DOX** could be observed by UPLC-MS. **28c** was diluted under tumour-like conditions for 3 d to release **DOX** in a sophisticated defurylation reaction (Figure 9, c).^[39]

To further increase the scope of potential drugs for mechanochemical release and to transition from an intermolecular to a kinetically superior intramolecular release system, Göstl and Herrmann introduced a variety of carbonate-based linkers which are in β -position to a disulfide mechanophore (Figure 10).^[43]

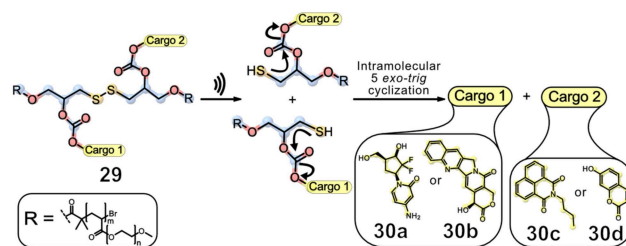


Figure 10. The force-induced intramolecular release of drugs from β -carbonate disulfide mechanophores. The generated thiols underwent intramolecular 5-*exo-trig* cyclisation, releasing the cargo and greatly accelerating the process compared to intermolecular systems.^[43]

The labile disulfide bond was cleaved using ultrasound, resulting in an intramolecular 5-*exo-trig* cyclisation to release the desired cargo. In this study, both the force-induced release of fluorophore umbelliferone (**30d**) and camptothecin (**30b**), an inhibitor of topoisomerase I and hence an anti-cancer drug,^[44] were achieved by sonicating the polymeric scaffold **29** for 4 h (20 kHz, ca. 16 W cm⁻²). UV/Vis and fluorescence spectroscopy demonstrated bond cleavage of the disulfide bond and a release of approximately 80% was calculated for UMB benchmarking the release efficiency of the system for hydroxy-bearing drugs. The released drug CPT was then incubated with HeLa cells, showing a notable increase in cytotoxicity after sonication compared to the polymer-bound carrier system.

Because of the β -carbonate polymer's bifunctional character, a fluorophore (**30a** and **30b**) can be released alongside the drug (**30c** and **30d**), rendering theranostic drug release possible.^[45] Therefore, the groups of Herrmann and Göstl released *N*-butyl-4-hydroxy-1,8-naphthalimide (**30c**) alongside **30b** and **30d** alongside gemcitabine (**30a**) by ultrasonication. Investigation of the diagnostic behaviour of polymer **29** in HeLa cells suggests that **30c** quickly diffuses into the cell after sonication. The mechanochemical activation was further monitored by MTS proliferation assays. A decrease in cell viability during ex situ sonication confirmed the successful release of **30b**, indicating a correlation between the activation of **30b** and the survival rate of the cell. To demonstrate the versatility of this method, an exchange of the drug (**30b**) and the fluorophore (**30c**) through **30d** and **30a** was conducted, resulting in a release of 55% after 4 h of sonication. As a nucleoside analogue, **30a** replaces cytidine during DNA replication, which results in cell death.^[46] This strategy was then adapted from hydroxy-bearing cargo molecules to amine-functionalities, further expanding the drug and fluorophore scope, although the release of amines from their carbamate derivatives was considerably slower and occasionally less efficient after mechanochemical disulfide scission compared to the carbonate counterparts.^[47]

Another approach for drug activation by ultrasound relies on the binding of cargo to polyaptamer (P_{APT}) polynucleotides. While single aptamers (APT) bind cargo efficiently, they cannot be activated by force due to their comparatively short contour length. Using the sequence of an aptamer in combination with rolling circle amplification/transcription (RCA/RCT) allows access

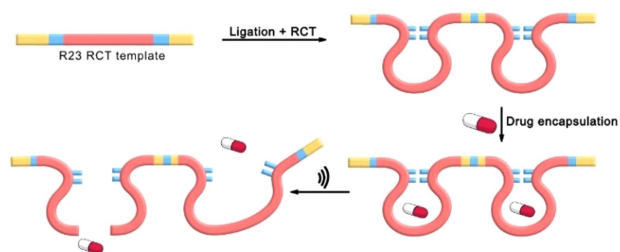


Figure 11. Polyaptamers were prepared by an RCT process bearing multiple cargo binding sites in their backbone. Ultrasonication stretches and fragments the polyaptamers, releasing the drug cargo.^[43]

to ultra-high molar mass polynucleotides (millions of base pairs) that bind multiple cargo molecules along the chain (Figure 11).

As a result, R23 RNA polyaptamers^[48] were created for binding the antibiotics neomycin B or paromomycin.^[43] Gel electrophoresis and agar tests confirmed the strong incorporation of the antibiotics into the complex. In the following sonication experiments, a cargo release of approximately 80% after 30 min could be achieved, which was quantified by ImageJ. Minimal inhibitory concentration (MIC) tests against *S. aureus* suggest that antibacterial properties can only be achieved with pristine neomycin B or the sonicated polyaptamers containing neomycin B, but not with the single aptamer complex.

Polyaptamers can also complex and inhibit the catalytic activity of enzymes, such as shown for thrombin, which is vital for secondary hemostasis.^[49] Therefore, TBA₁₅ polyaptamers were produced by RCA which then captured thrombin and inhibited its activity through the formation of a well-defined aptamer-protein complex. Ultrasonication for a few minutes released the thrombin, restoring its catalytic activity. Importantly, for the first time, the groups of Herrmann, Göstl, and Kießling demonstrated the use of clinically established low-intensity focused ultrasound (LIFU) at 5 MHz for six minutes. This brings clinical application of such drug delivery and release platforms closer to application.

4. Metallopolymer-Based Systems

4.1. Metal-ion release

The group of Sijbesma investigated whether the release of metal ions from a mechanophore can be used for applications, such as reaction catalysis by mechanochemical activation of latent catalysts.^[50–53] In a fundamental work, the researchers synthesized various silver complexes that are coordinated by polymer-substituted NHC ligands **31 a–b** (Figure 12, a). These were shown to be quite active mechanophores and sonication in MeCN with H₂O (0.1% v/v) resulted in the conversion of the Ag-NHC complex into the imidazolium salt in 49% yield.

Traces of H₂O were necessary to observe scission, since recoordination of dissociated ligands to the metal needed to be suppressed. After the addition of CS₂ to the wet solvent, the

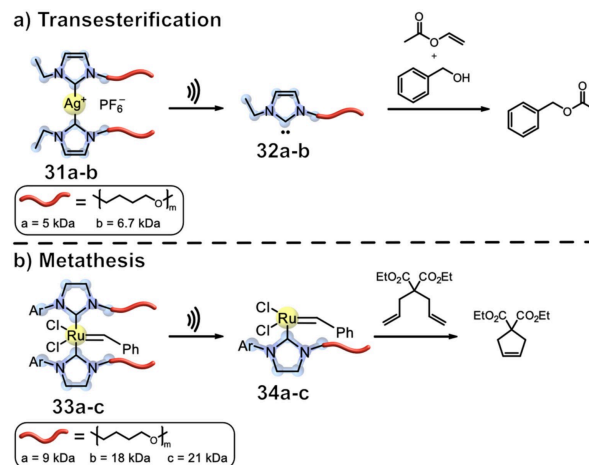


Figure 12. Polymer-substituted NHC ligands **31 a–b** & **33 a–c** for reaction catalysis by mechanochemical activation of latent catalysts. a) Activation of Ag-NHC complexes **31 a–b** enabled transesterification reactions catalysed by free carbenes and Ag⁺ b) polymer-bound, Grubbs-like Ru-catalysts **33 a–c** activated mechanochemically allowed for substrate coordination and subsequent ring-closing metathesis (RCM) reactions.^[51]

conversion could be improved to 99%, rendering this system suitable for targeted metal ion release.^[50] However, the role of CS₂ remained unclear. The following works described catalysts that can be activated by mechanical force generated by ultrasound. Catalysts based on Ag-NHC complexes, exploiting the previously described system and complemented by Ru Grubbs-like catalysts, were investigated that allowed for different organic transformations such as transesterification and olefin metathesis. Transesterification of vinyl acetate and benzyl alcohol was achieved in a modest conversion of 65% for the first time by mechanochemical catalyst activation, attributed to the liberated NHCs during the sonication process and their catalytic activity for transesterification. While this again demonstrates the successful metal ion release, the reaction must not necessarily be metal catalysed, as carbenes are known to catalyse transesterification as well.^[54] The reactions were run using neat reagents without explicitly adding H₂O to suppress free carbenes, in contrast to the former experiments.^[51] To demonstrate the activation of a metal catalyst by means of a sonochemical stimulus, Sijbesma and co-workers designed a polymer-centred, Grubbs-like Ru-catalyst **33 a–c** (Figure 12, b). Ru alkylidene complexes are catalysts for ROMP and RCM reactions. The catalytic activity of these complexes is restrained through the bis complexation by the NHC polymeric ligands. During sonication, bond scission occurs at the NHC–Ru bond, activating the catalytic behaviour of the Ru-benzylidene complex. The RCM of diethyl diallylmalonate with the mechanophore **33 a–c** resulted in a conversion of 14% after 2 h. To improve the yield, an increase in polymer length to facilitate scission was envisioned. The significantly higher *M_n* led to a conversion of 36% under the same reaction conditions, suggesting an influence of the polymer length in relation to its mechanochemical activation. To demonstrate the universality of this dissociation-induced catalyst, a final ROMP of cyclooctene

with mechanophore **33c** was performed. The increased M_n of roughly 21 kDa per chain moiety made the mechanochemical activation efficient and resulted in more scission concomitant with more active catalyst available. A total conversion of 90% into polyoctenamer could be observed, though the D_M of 1.6 was rather high. This is consistent with the group's proposed mechanism since the slow release of the catalytically active centrum is an ongoing process during sonication, hence violating the prerequisites of controlled polymerisation ($R_i \gg R_p$).

Although the previous paragraphs focused primarily on metal ion release and its applications and mechanisms, it is important to introduce Diesendruck and co-workers' innovative work, in which intramolecular self-repair of chemical bonds induced by mechanochemical bond scission was demonstrated.^[55] A polybutadiene polymer was used in combination with *g*DCC, which acts as an internal indicator for the magnitude of bond scission during sonication. When $Rh_2Cl_2(C_2H_4)_4$ is added to a highly diluted polymer solution, single-chain polymer nanoparticles (SCNPs) **35** are formed, with the polymer chains interconnected intramolecularly via numerous Rh- π bonds. Several SCNPs were synthesized for sonication experiments, each with a different amount of Rh^I complex added, and thus a different level of intrachain cross-linking (Figure 13). As anticipated, a decrease in the hydrodynamic volume was observable with increasing amounts of added Rh^I. Sonication of the linear polymer and the slightly cross-linked polymers (0.5–1%) resulted in an activation of 60% of the *g*DCC mechanophores. With an increasing amount of cross-linking, the *g*DCC activation could be reduced to 10% due to the preferred bond scission of the Rh- π complex. Instead of chain fragmentation, this Rh- π bond breakage resulted in polymer chain unfolding (**36**). This mechanochemical unfolding process was reversible, making it possible to autonomously repair broken bonds (**37**). This was demonstrated in sonication experiments with different pulse intervals (1–16 s), showing that a longer interval time allows the polymer to refold and cross-link. The activation of *g*DCC could be reduced by approximately 50%, indicating the significance of the cross-linkage and the sonication interval time.^[55]

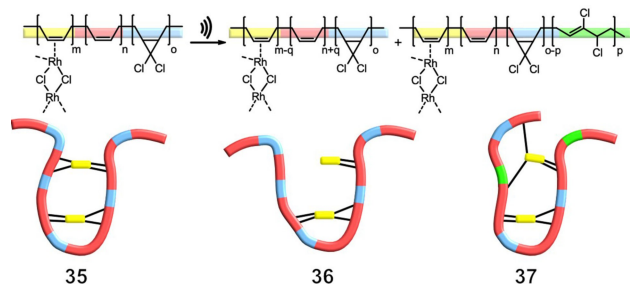


Figure 13. Intramolecular cross-linking by Rh- π bonds led to controlled unfolding of the polymer under stress in solution, showing that mechanical stress can be removed from the polymer backbone and successfully transferred onto the weaker intrachain cross-links. Linear polybutadiene was functionalized by cycloaddition of dichlorocarbene to the double bonds, giving *g*DCC mechanophores in the backbone. Base quantities were tuned to provide a conversion of 45% with butadiene units remaining unreacted for subsequent rhodium coordination.^[55]

4.2. Metallocenes

In recent years, a new class of mechanophores has been developed, using various metallocene derivatives in main-chain polymers to undergo bond scission, cumulating in metal ion release (Figure 14).^[2c]

Weder, Fromm, and co-workers reported the first ferrocene (Fc) PMA-centred **38**, synthesized through Cu⁰-catalyzed controlled radical polymerization yielding a chain with a M_n of 133 kDa.^[56] Upon ultrasonication, the group discovered a M_n decrease of **38** by nearly 50%, which they attributed to a preferential chain cleavage at the metal centre (Figure 15). In contrast, the control mechanophore (without Fc) was observed to have a much lower chain scission rate. To demonstrate unequivocally that the chain cleavage occurs at the Fc moiety of **38**, KSCN was added to the sonicated solution, resulting in the formation of a red complex $[Fe(SCN)_n(H_2O)_{6-n}]^{(3-n)+}$ with the released Fe³⁺, as confirmed by UV/Vis spectroscopy. Different control experiments with 1,1'-ferrocenedimethanol, a low-molar-mass polymer, and a monofunctionalized polymer indicated no release of Fe³⁺ ions, and therefore no colour change occurred, confirming that the main chain scission occurred at the Fc itself. To further increase the amount of released Fe³⁺, Weder, Fromm, and co-workers synthesized a PU-based network in a polycondensation reaction. This PU contained several Fc mechanophores, randomly distributed over the polymer backbone to ensure that during ultrasonication, multiple Fc entities can be cleaved. With a higher release of Fe³⁺ ions from the polyurethane mechanophore, a significantly lower polymer concentration (0.75 mg mL⁻¹) was needed to detect the formed red

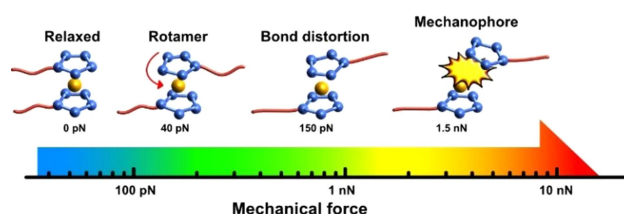


Figure 14. Metallocenes are unique mechanophores undergoing several intramolecular changes. This depends on the magnitude of force exerted on the system.^[2c]

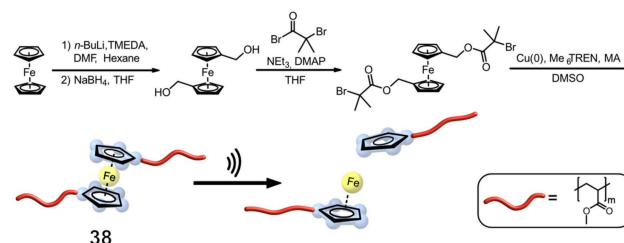


Figure 15. Fc-containing bifunctional initiator bearing methyl α -bromoisobutyrate was used to prepare **38** and a reference polymer (not depicted) with M_n of 133 and 119 kDa, respectively, and a narrow D_M of 1.1. Scission of the Fc mechanophore in a PMA backbone is at least 10 \times more favoured than non-specific cleavage and leads to Fe³⁺ release.^[56]

thiocyanate complex by UV/Vis spectroscopy, compared to the PMA mechanophore (2 mg mL^{-1}).

During sonication, both specific bond scission and random chain cleavage were observed for PMA and PU. To gain a better understanding of the reaction kinetics, Weder, Fromm, and co-workers created a model that distinguishes between specific and non-specific chain scission. As a result, kinetic equations for the concentration of polymer chains of various lengths had to be used. The “population balance equations” approach takes several factors into account in the event of chain cleavage. For example, the localization of the mechanophore in the polymer, the fragment distribution, and kinetic constants which describe the rate of bond scission of the Fc units. These kinetic constants (k_1 and k_2) change over time, since the polymer chains get shorter with each bond cleavage. For **38** (Fc in PMA) $k_2 = 0.0064 \text{ min}^{-1}$ defines the non-specific bond cleavage. In contrast, $k_1 = 0.058 \text{ min}^{-1}$ describes the event of specific bond scission at the Fc moiety and is approximately $10\times$ more probable.^[56] Following these results, Tang, Craig, and co-workers investigated the specific bond cleavage in more detail and examined whether the reaction occurred in a homolytic or heterolytic fashion.^[57] Therefore, they synthesized several polymers which varied both in length and number of mechanophores, using entropy-driven (ED) ROMP. In a first sonication experiment using **39a**, an increase in signals corresponding to the cyclopentadienyl (Cp) ligand was observed by ^1H NMR. It was hypothesized that the Cp ligand was formed during sonication from a cyclopentadienyl anion. The addition of isopropyl alcohol to the solution resulted in a significant increase in signals corresponding to the ligand, indicating that the Cp ligand was formed by protonation. This result would support the assumption that the Cp bond cleavage follows a heterolytic mechanism where Cp^- dissociates from $[\text{CpFe}]^+$. For further investigations, gDCC mechanophores were incorporated into the polymer, serving as an internal standard to quantify the mechanical bond strength of Fc (Figure 16). During sonication, the amount of gDCCs ring-opening per scission cycle, ϕ_{ir} , provided information about the relative mechanochemical bond strength.

When three different polymers were compared, it was discovered that ϕ_i of **39b** ($\phi_i = 0.22$) is noticeably lower than that of the polybutadiene polymer **40** ($\phi_i = 0.79$) and the aryl ester polymer **41** ($\phi_i = 0.62$) both of which lack the Fc moiety.

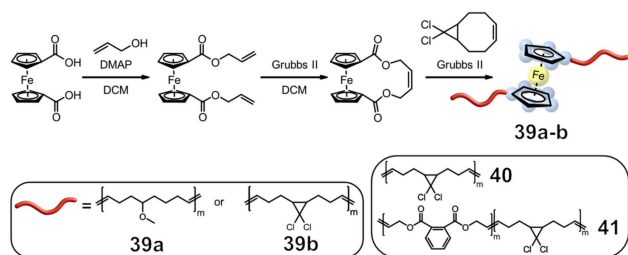


Figure 16. Representative synthetic scheme for Fc-containing polymers used in the study of Craig, Tang and co-workers, exemplarily showing gDCC.^[57]

These results demonstrate the high mechanical activity of the Fe–Cp interaction in contrast to the carbon-carbon bonds.

If the mechanism of the dissociation was heterolytic, as the first experiments indicated, the stabilization of the charge separation of Cp^- and $[\text{CpFe}]^+$ through an organic salt should be detectable. As anticipated, the addition of $\text{Bu}_4\text{N}^+\text{Br}^-$ further reduced ϕ_i of **39b** from $\phi_i = 0.22$ to $\phi_i = 0.12$ consistent with a heterolytic mechanism. This fine-tuning with $\text{Bu}_4\text{N}^+\text{Br}^-$ is specific to polymers with metallocenes, as seen in a control experiment with **40**, and increases the mechanoresponsive sensitivity.^[57]

The groups of Tang and Craig investigated the influence of the central metal atom on the mechanophore in addition to the previous results. ED-ROMP was used to create a polymer similar to **39_{Fc}** (polymer with Fc) but with ruthenocene (Rc) **39_{Rc}** instead of Fc.^[58] In comparison, the mechanical strength of the Rc mechanophore **39_{Rc}** ($\phi_i = 0.43$) was found to be significantly higher than that of Fc **39_{Fc}** ($\phi_i = 0.22$). The CoGEF calculations give a good understanding of the two-step dissociation process and why Rc has a higher mechanical strength of **39_{Rc}** ($\phi_i = 0.43$) in comparison to Fc **39_{Fc}** ($\phi_i = 0.22$) (Figure 17).^[58]

In contrast to prior studies, the exchange of ruthenium to cobalt led to a destabilization of the control mechanophore attributed to the functional groups of the Cp-ligand and the positively charged Co centre. The electron withdrawing effect of the previous used ester linkages reduced the electron density of the Cp-ligand and led to a decrease in the Co–Cp interaction. In a sonication experiment for this control mechanophore decomposition was observed by ^1H NMR and ^{19}F NMR.

Craig and co-workers utilized electron-donating groups (EDG) for future experiments based on polyoctene chains,

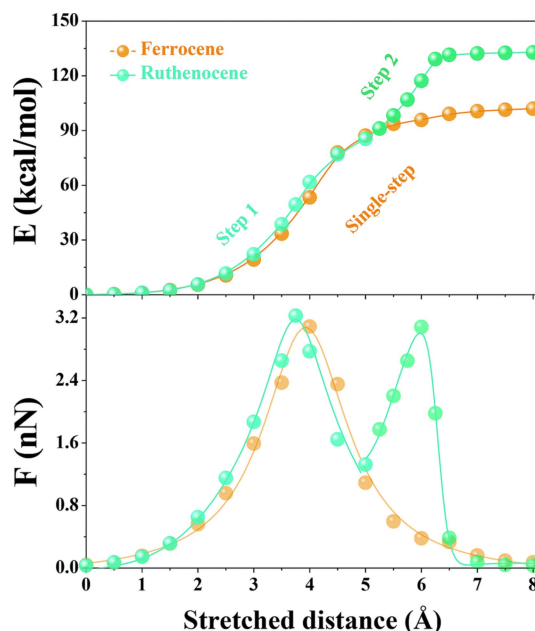


Figure 17. CoGEF-computed potential (top) and force (bottom) as a function of the stretching distance for Fc (orange dots) and Rc (turquoise dots).^[58] Reproduced from Ref. [58] with permission. Copyright 2021, Royal Society of Chemistry.

synthesized by a sequence of RCM and ROMP reactions. An additional advantage of these polymers is the absence of further functional groups, lowering the chance of secondary bond scission. Sonication experiments showed that a decrease of roughly 30% of M_n could be achieved after 2 h for the embedded cobaltocene (Cc) mechanophore. ^1H NMR confirmed that, similar to previous metallocenes, a decrease of Cp-ligands occurred and terminal Cp was formed. ^{19}F NMR verified that bond scission occurred preferably at the Rc moiety due to a decrease of PF_6^- .

As proven previously, the cleavage of a metallocene follows a heterolytic dissociation, suggesting that Cc would follow the same mechanism and that the cobalt ion would maintain its oxidation state of +3 after sonication. The addition of 1,10-phenanthroline trapped released metal ions by forming a charge transfer complex, which could be detected by UV/Vis. As anticipated, after sonication, an absorption peak at 325 nm could be observed for $[\text{Co}(\text{phenanthroline})_3]^{3+}$, again confirming a heterolytic mechanism. Since Cc differs structurally with its counterion from the previously discussed neutral metallocene, an additional examination of the CoGEF method gave further insight into the moment of bond cleavage during sonication. While the Cp rings were getting “peeled off” from the sandwich structure, they simultaneously allowed an attractive interaction between the Co cation and PF_6^- anion. In comparison to Fc, this interaction facilitated bond cleavage and made it a more sensitive mechanophore.^[59] The influence of different aspects during bond scission was discussed and a difference between a slipping and peeling mechanism was observed. For a slipping mechanism to occur, Cp ligand rotation is crucial. Craig and co-workers reasoned that *ansa*-bridging (adding a linking group between the two Cp rings to form an interannular bridge) of the Cp ligands could force the Fc slipping mechanism into a peeling pathway, increasing its mechanochemical reactivity (Figure 18).

Single-molecule force spectroscopy (SMFS) revealed that *cis-42₃* would dissociate $10^7\times$ faster than unbridged Fc. During this process, the dihedral angle increased over time, “ripping” off the Cp ligand from the mechanophore. This mechanism could only be observed for the *cis*-mechanophores (Figure 19). The ferrocene without an *ansa*-bridge and the *trans-42₃*

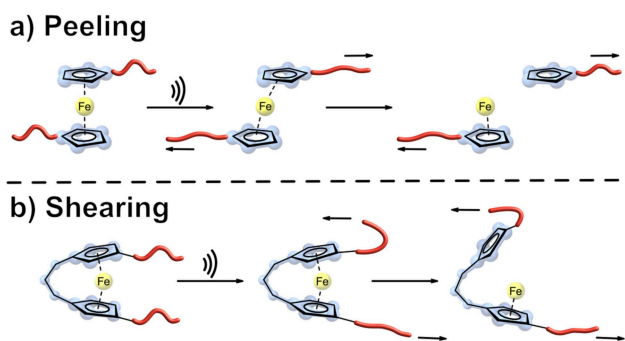


Figure 18. a) Force-induced bond scission of a metallocenes following a peeling mechanism; b) conformational restrictions in *ansa*-type metallocenes lead to a shearing mechanism.^[60]

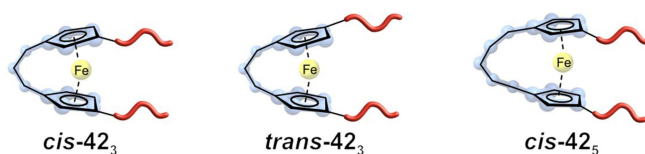


Figure 19. Three different *ansa*-bridged Fc-based mechanophores. *Cis-42₃*, *trans-42₃* and *cis-42₅* (f. l. t. r.), with *cis-42₅* having the lowest ring-strain.^[60] *Cis-42₃* shows a dissociation rate constant increase of several orders of magnitude due to the *ansa*-bridge.

showed an increase in the dihedral angle between the attached polymer chains. For *trans-42₃*, this behaviour resembled the earlier discussed slippage mechanism of Fc with a combination of the “peeling” process.

These mechanistic differences can be used for bulk materials to tune their individual force-responsive behaviour. Therefore, Fc and *cis-42₃* were respectively integrated into elastomers. As before, phenanthroline was added to trap emerging Fe^{2+} metal ions to form a red complex for UV/Vis spectroscopy. A drop test for both mechanophores showed that a higher release of Fe^{2+} for *cis-42₃* (1% activated) was achieved, resulting in a deeper red colour ($\lambda_{\text{max}} \approx 520$ nm) in contrast to the Fc incorporated polymer (0.4% activated). This behaviour was attributed to the previous described *ansa*-bridging and mechanistic changes.^[60]

4.3. Supramolecular cage-based systems

The group of Schmidt in cooperation with the group of Göstl reported the activation of a cargo-carrying supramolecular *exo*-functionalized Pd cage.^[61] The octahedral cage-like assembly,^[62] bears polymer chains on each vertex and is comprised of 4 triangular panels, 6 Pd atoms, and 6 bpy units, leading to the formation of a star-shaped poly(ethylene glycol) methyl ether (PEG) polymer, with the self-assembled cage in the centre (Figure 20). The system is unique, as the star-shaped polymer is constructed during the self-assembly of the bipyridine-based Pd^{II} precursors with the organic triazine panels, employing the same Pd–N bonds that later were used for force-induced

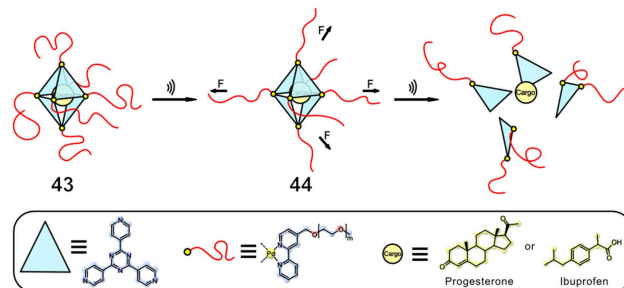


Figure 20. The *exo* PEG-functionalized octahedral cage **43** has an X_n of 220 repetitive ethylene glycol units connected to each vertex, resulting in a total M_n of 60 kDa. When activated by ultrasound in aqueous solution, the cage fragmented, releasing the non-covalently bound, preloaded cargo from its hydrophobic cavity.^[61]

scission. Hydrophobic guests, unmodified progesterone or two molecules of ibuprofen, could be taken up per supramolecular entity. Sonication experiments on the cargo-loaded cage **43** were carried out in H₂O with an immersion probe sonicator (20 kHz, 6 h, 1 s on and 1 s off cycles), leading to complete cargo release in both cases. This system represents the first example of a supramolecular coordination cage forming a star-shaped, water-soluble polymer structure that responds to ultrasonication-induced shear force in solution, allowing for utilization of the hydrophobic nanocavity inside.^[62]

5. Conclusion

The responsive release systems highlighted here are proof-of-concept studies that may suffer from multi-step synthesis, low mechanochemical sensitivity, and poor drug delivery efficiency. Nevertheless, these nanomaterials show very promising potential to realize controllable release or activation of their cargo in diverse applications in the future.

Boydston and co-workers as well as Craig and co-workers have elegantly demonstrated this with the principle of flex activation, yet such systems show low release efficiencies, suffer from limited cargo scope, and were not shown to be usable in solution. Specifically, the groups of Robb, Herrmann, and Göstl developed solutions for the highly efficient release of a wide cargo scope employing cascade release reactions. However, in such systems, the actual release process is only indirectly coupled to the force-dependent step and hence can vary among cargo molecules. Virtually any hydrophobic pristine cargo can be incorporated into the metal-organic cages prepared by Schmidt, Göstl, and co-workers, although in the future, the syntheses need to be facilitated and the mechanochemical reaction times optimized. In addition, all systems mentioned above suffer from very low cargo loading fractions, as expressed in the amount of cargo per polymer mass. This issue can be attenuated by producing multimechanophore architectures, such as performed for H⁺-release from gDCC by Craig and co-workers. In particular, polyaptamers are interesting in this regard since they can be prepared for virtually any compound and, due to their very high molar mass, are highly active under force. Yet, the comparably high costs associated with polynucleic acid synthesis can hold back application of such systems in bulk quantities.

In summary, we have highlighted functional macromolecular systems, in which the incorporation of mechanophores enables application of external force to be used to control their functionality, with our focus lying on cargo release systems. We hope that this review of a thriving and vibrant topic with a plethora of possibilities will encourage and enable further multidisciplinary collaboration of engineers and scientists from fields such as chemistry, biology, engineering, medicine, nanotechnology, and materials science.

Acknowledgements

We thank the Strategic Research Fund of Heinrich Heine University (F-2018/1460-4), the Manchot Foundation for a fellowship to R.K., and the North Rhine-Westphalian Academy of Sciences, Humanities and the Arts (B.M.S.). R.G. is thankful for a Freigeist-Fellowship of the Volkswagen Foundation (92888). Open Access funding enabled and organized by Projekt DEAL.

Conflict of Interest

The authors declare no conflict of interest.

Data Availability Statement

Data sharing is not applicable to this article as no new data were created or analyzed in this study.

Keywords: drug release · mechanochemistry · polymers · sonochemistry · ultrasound

- [1] a) S. Panja, D. J. Adams, *Chem. Soc. Rev.* **2021**, *50*, 5165–5200; b) J. M. McCracken, B. R. Donovan, T. J. White, *Adv. Mater.* **2020**, *32*, 19906564; c) G. Kocak, C. Tuncer, V. Bütün, *Polym. Chem.* **2017**, *8*, 144–176; d) M. D. Segarra-Maset, V. J. Nebot, J. F. Miravet, B. Escuder, *Chem. Soc. Rev.* **2013**, *42*, 7086–7098; e) J. Thévenot, H. Oliveira, O. Sandre, S. Lecommandoux, *Chem. Soc. Rev.* **2013**, *42*, 7099–7116; f) L. Sun, W. M. Huang, Z. Ding, Y. Zhao, C. C. Wang, H. Purnawali, C. Tang, *Mater. Des.* **2012**, *33*, 577–640.
- [2] a) R. T. O'Neill, R. Boulatov, *Nat. Chem. Rev.* **2021**, *5*, 148–167; b) M. A. Ghanem, A. Basu, R. Behrou, N. Boechler, A. J. Boydston, S. L. Craig, Y. Lin, B. E. Lynde, A. Nelson, H. Shen, D. W. Storti, *Nat. Rev. Mater.* **2021**, *6*, 84–98; c) Y. Sha, H. Zhang, Z. Zhou, Z. Luo, *Polym. Chem.* **2021**, *12*, 2509–2521; d) Y. Chen, G. Mellot, D. van Luijk, C. Creton, R. P. Sijbesma, *Chem. Soc. Rev.* **2021**, *50*, 4100–4140; e) M. Stratigaki, R. Göstl, *ChemPlusChem* **2020**, *85*, 1095–1103; f) E. Izak-Nau, D. Campagna, C. Baumann, R. Göstl, *Polym. Chem.* **2020**, *11*, 2274–2299; g) B. H. Bowser, S. L. Craig, *Polym. Chem.* **2018**, *9*, 3583–3593; h) G. De Bo, *Chem. Sci.* **2018**, *9*, 15–21; i) S. Akbulatov, R. Boulatov, *ChemPhysChem* **2017**, *18*, 1422–1450; j) Y. Zhang, J. Yu, H. N. Bomba, Y. Zhu, Z. Gu, *Chem. Rev.* **2016**, *116*, 12536–12563; k) C. L. Brown, S. L. Craig, *Chem. Sci.* **2015**, *6*, 2158–2165; l) J. Li, C. Nagamani, J. S. Moore, *Acc. Chem. Res.* **2015**, *48*, 2181–2190; m) P. A. May, J. S. Moore, *Chem. Soc. Rev.* **2013**, *42*, 7497–7506; n) R. Groote, R. T. M. Jakobs, R. P. Sijbesma, *Polym. Chem.* **2013**, *4*, 4846–4859; o) A. L. Black, J. M. Lenhardt, S. L. Craig, *J. Mater. Chem.* **2011**, *21*, 1655–1663; p) M. M. Caruso, D. A. Davis, Q. Shen, S. A. Odom, N. R. Sottos, S. R. White, J. S. Moore, *Chem. Rev.* **2009**, *109*, 5755–5798; q) J. M. J. Paulusse, R. P. Sijbesma, *J. Polym. Sci. Part A* **2006**, *44*, 5445–5453; r) S. He, M. Stratigaki, S. P. Centeno, A. Dreuw, R. Göstl, *Chem. Eur. J.* **2021**, *27*, 15889–15897; s) H. Traeger, D. J. Kiebal, C. Weder, S. Schrettl, *Macromol. Rapid Commun.* **2021**, *42*, 2000573.
- [3] a) A. Goulet-Hanssens, F. Eisenreich, S. Hecht, *Adv. Mater.* **2020**, *32*, 1905966; b) J. Boelke, S. Hecht, *Adv. Opt. Mater.* **2019**, *7*, 1900404; c) F. Lancia, A. Ryabchun, N. Katsonis, *Nat. Chem. Rev.* **2019**, *3*, 536–551; d) L. Wang, Q. Li, *Chem. Soc. Rev.* **2018**, *47*, 1044–1097; e) S. Chatani, C. J. Kloxin, C. N. Bowman, *Polym. Chem.* **2014**, *5*, 2187–2201.
- [4] See the following editorials as introductions to mechanochemistry: a) R. Boulatov, *ChemPhysChem* **2017**, *18*, 1419–1421; b) S. L. Craig, *Nat. Chem.* **2017**, *9*, 1154; c) S. L. James, T. Friščić, *Chem. Soc. Rev.* **2013**, *42*, 7494–7496; d) J. G. Hernández, *Beilstein J. Org. Chem.* **2017**, *13*, 2372–2373; e) J. G. Hernández, *Beilstein J. Org. Chem.* **2019**, *15*, 1521–1522.
- [5] K. S. Suslick, *Faraday Discuss.* **2014**, *170*, 411–422.
- [6] J. M. Lenhardt, A. L. B. Ramirez, B. Lee, T. B. Kouznetsova, S. L. Craig, *Macromolecules* **2015**, *48*, 6396–6403.

- [7] a) J. Wang, T. B. Kouznetsova, Z. S. Kean, L. Fan, B. D. Mar, T. J. Martínez, S. L. Craig, *J. Am. Chem. Soc.* **2014**, *136*, 15162–15165; b) G. R. Gossweiler, T. B. Kouznetsova, S. L. Craig, *J. Am. Chem. Soc.* **2015**, *137*, 6148–6151.
- [8] S. Y. Lee, Y. Lee, J. E. Kim, T. G. Park, C.-H. Ahn, *J. Mater. Chem.* **2009**, *19*, 8198–8201.
- [9] S. Binauld, M. H. Stenzel, *Chem. Commun.* **2013**, *49*, 2082–2102.
- [10] H.-H. Liu, W.-T. Chen, F.-C. Wu, *J. Polym. Res.* **2002**, *9*, 251–256.
- [11] a) C. Fu, J. Xu, C. Boyer, *Chem. Commun.* **2016**, *52*, 7126–7129; b) D. Delcroix, B. Martín-Vaca, D. Bourissou, C. Navarro, *Macromolecules* **2010**, *43*, 8828–8835.
- [12] C. E. Diesendruck, B. D. Steinberg, N. Sugai, M. N. Silberstein, N. R. Sottos, S. R. White, P. V. Braun, J. S. Moore, *J. Am. Chem. Soc.* **2012**, *134*, 12446–12449.
- [13] C. Nagamani, H. Liu, J. S. Moore, *J. Am. Chem. Soc.* **2016**, *138*, 2540–2543.
- [14] E. E. Schweizer, W. E. Parham, *J. Am. Chem. Soc.* **1960**, *82*, 4085–4087.
- [15] Y. Lin, T. B. Kouznetsova, S. L. Craig, *J. Am. Chem. Soc.* **2020**, *142*, 99–103.
- [16] a) D. Schilter, *Nat. Chem. Rev.* **2020**, *4*, 505; b) J. Gurke, Š. Budzák, B. M. Schmidt, D. Jacquemin, S. Hecht, *Angew. Chem. Int. Ed.* **2018**, *57*, 4797–4801; *Angew. Chem.* **2018**, *130*, 4888–4893.
- [17] D. A. Davis, A. Hamilton, J. Yang, L. D. Cremer, D. Van Gough, S. L. Potisek, M. T. Ong, P. V. Braun, T. J. Martínez, S. R. White, J. S. Moore, N. R. Sottos, *Nature* **2009**, *459*, 68–72.
- [18] M. B. Larsen, A. J. Boydston, *J. Am. Chem. Soc.* **2013**, *135*, 8189–8192.
- [19] J. Kost, K. Leong, R. Langer, *Proc. Natl. Acad. Sci. USA* **1989**, *86*, 7663–7666.
- [20] a) Y. Liu, S. Holm, J. Meisner, Y. Jia, Q. Wu, T. J. Woods, T. J. Martínez, J. S. Moore, *Science* **2021**, *373*, 208–212; b) C. L. Brown, B. H. Bowser, J. Meisner, T. B. Kouznetsova, S. Seritan, T. J. Martínez, S. L. Craig, *J. Am. Chem. Soc.* **2021**, *143*, 3846–3855; c) I. M. Klein, C. C. Husic, D. P. Kovács, N. J. Choquette, M. J. Robb, *J. Am. Chem. Soc.* **2020**, *142*, 16364–16381.
- [21] J. M. Lenhardt, A. L. Black, B. A. Beiermann, B. D. Steinberg, F. Rahman, T. Samborski, J. Elsaker, J. S. Moore, N. R. Sottos, S. L. Craig, *J. Mater. Chem.* **2011**, *21*, 8454–8459.
- [22] M. B. Larsen, A. J. Boydston, *J. Am. Chem. Soc.* **2014**, *136*, 1276–1279.
- [23] Z. S. Petrović, I. Javni, G. Bánhegy, *J. Polym. Sci. B Polym. Phys.* **1998**, *36*, 221–235.
- [24] a) C. P. Buckley, C. Prisacariu, C. Martin, *Polymer* **2010**, *51*, 3213–3224; b) J. Yi, M. C. Boyce, G. F. Lee, E. Balizer, *Polymer* **2006**, *47*, 319–329.
- [25] D. M. Flanigan, F. Romanov-Michailidis, N. A. White, T. Rovis, *Chem. Rev.* **2015**, *115*, 9307–9387.
- [26] H. Shen, M. B. Larsen, A. G. Roessler, P. M. Zimmerman, A. J. Boydston, *Angew. Chem. Int. Ed.* **2021**, *60*, 13559–13563; *Angew. Chem.* **2021**, *133*, 13671–13675.
- [27] P. B. Jayathilaka, T. G. Molley, Y. Huang, M. S. Islam, M. R. Buche, M. N. Silberstein, J. J. Kruzic, K. A. Kilian, *Chem. Commun.* **2021**, *57*, 8484–8487.
- [28] a) B. A. Beiermann, S. L. B. Kramer, J. S. Moore, S. R. White, N. R. Sottos, *ACS Macro Lett.* **2012**, *1*, 163–166; b) Y. Chen, A. J. Spiering, S. Karthikeyan, G. W. Peters, E. W. Meijer, R. P. Sijbesma, *Nat. Chem.* **2012**, *4*, 559–562; c) D. Yildiz, C. Baumann, A. Mikosch, A. J. C. Kuehne, A. Herrmann, R. Göstl, *Angew. Chem. Int. Ed.* **2019**, *58*, 12919–12923; *Angew. Chem.* **2019**, *131*, 13051–13055.
- [29] a) S. L. Potisek, D. A. Davis, N. R. Sottos, S. R. White, J. S. Moore, *J. Am. Chem. Soc.* **2007**, *129*, 13808–13809; b) D. A. Davis, A. Hamilton, J. Yang, L. D. Cremer, D. Van Gough, S. L. Potisek, M. T. Ong, P. V. Braun, T. J. Martínez, S. R. White, J. S. Moore, N. R. Sottos, *Nature* **2009**, *459*, 68–72.
- [30] C. K. Lee, B. A. Beiermann, M. N. Silberstein, J. Wang, J. S. Moore, N. R. Sottos, P. V. Braun, *Macromolecules* **2013**, *46*, 3746–3752.
- [31] G. O'Bryan, B. M. Wong, J. R. McElhanon, *ACS Appl. Mater. Interfaces* **2010**, *2*, 1594–1600.
- [32] N. Roy, J.-M. Lehn, *Chem. Asian J.* **2011**, *6*, 2419–2425.
- [33] G. R. Gossweiler, G. B. Hewage, G. Soriano, Q. Wang, G. W. Welshofer, X. Zhao, S. L. Craig, *ACS Macro Lett.* **2014**, *3*, 216–219.
- [34] Y. Lu, H. Sugita, K. Mikami, D. Aoki, H. Otsuka, *J. Am. Chem. Soc.* **2021**, *143*, 17744–17750.
- [35] J. Wang, T. B. Kouznetsova, R. Boulatov, S. L. Craig, *Nat. Commun.* **2016**, *7*, 13433.
- [36] X. Hu, T. Zeng, C. C. Husic, M. J. Robb, *J. Am. Chem. Soc.* **2019**, *141*, 15018–15023.
- [37] X. Hu, T. Zeng, C. C. Husic, M. J. Robb, *ACS Cent. Sci.* **2021**, *7*, 1216–1224.
- [38] T. Zeng, X. Hu, M. J. Robb, *Chem. Commun.* **2021**, *57*, 11173–11176.
- [39] Z. Shi, J. Wu, Q. Song, R. Göstl, A. Herrmann, *J. Am. Chem. Soc.* **2020**, *142*, 14725–14732.
- [40] M. L. Buck, *Pediatr. Pharmacol.* **2009**, *15*, 1–5.
- [41] J. Prandota, *Am. J. Ther.* **2001**, *8*, 275–289.
- [42] R. Injac, B. Strukelj, *Technol. Cancer Res. Treat.* **2008**, *7*, 497–516.
- [43] S. Huo, P. Zhao, Z. Shi, M. Zou, X. Yang, E. Warszawik, M. Loznik, R. Göstl, A. Herrmann, *Nat. Chem.* **2021**, *13*, 131–139.
- [44] R. P. Hertzberg, M. J. Caranfa, S. M. Hecht, *Biochemistry* **1989**, *28*, 4629–4638.
- [45] Z. Shi, Q. Song, R. Göstl, A. Herrmann, *Chem. Sci.* **2021**, *12*, 1668–1674.
- [46] a) Z. Yang, J. H. Lee, H. M. Jeon, J. H. Han, N. Park, Y. He, H. Lee, K. S. Hong, C. Kang, J. S. Kim, *J. Am. Chem. Soc.* **2013**, *135*, 11657–11662; b) M. H. Lee, J. L. Sessler, J. S. Kim, *Acc. Chem. Res.* **2015**, *48*, 2935–2946.
- [47] Z. Shi, Q. Song, R. Göstl, A. Herrmann, *CCS Chem.* **2021**, *3*, 2333–2344.
- [48] A. A. Bastian, A. Marcozzi, A. Herrmann, *Nat. Chem.* **2012**, *4*, 789–793.
- [49] P. Zhao, S. Huo, J. Fan, J. Chen, F. Kiessling, A. J. Boersma, R. Göstl, A. Herrmann, *Angew. Chem. Int. Ed.* **2021**, *60*, 14707–14714; *Angew. Chem.* **2021**, *133*, 14829–14836.
- [50] S. Karthikeyan, S. L. Potisek, A. Piermattei, R. P. Sijbesma, *J. Am. Chem. Soc.* **2008**, *130*, 14968–14969.
- [51] A. Piermattei, S. Karthikeyan, R. P. Sijbesma, *Nat. Chem.* **2009**, *1*, 133–137.
- [52] J. M. J. Paulusse, J. P. J. Huijbers, R. P. Sijbesma, *Chem. Eur. J.* **2006**, *12*, 4928–4934.
- [53] J. M. J. Paulusse, R. P. Sijbesma, *Angew. Chem. Int. Ed.* **2004**, *43*, 4460–4462; *Angew. Chem.* **2004**, *116*, 4560–4562.
- [54] N. Marion, S. Diez-González, S. P. Nolan, *Angew. Chem. Int. Ed.* **2007**, *46*, 2988–3000; *Angew. Chem.* **2007**, *119*, 3046–3058.
- [55] A. Levy, R. Feinstein, C. E. Diesendruck, *J. Am. Chem. Soc.* **2019**, *141*, 7256–7260.
- [56] M. Di Giannantonio, M. A. Ayer, E. Verde-Sesto, M. Lattuada, C. Weder, K. M. Fromm, *Angew. Chem. Int. Ed.* **2018**, *57*, 11445–11450; *Angew. Chem.* **2018**, *130*, 11616–11621.
- [57] Y. Sha, Y. Zhang, E. Xu, Z. Wang, T. Zhu, S. L. Craig, C. Tang, *ACS Macro Lett.* **2018**, *7*, 1174–1179.
- [58] Y. Sha, Y. Zhang, E. Xu, C. W. McAlister, T. Zhu, S. L. Craig, C. Tang, *Chem. Sci.* **2019**, *10*, 4959–4965.
- [59] Y. Cha, T. Zhu, Y. Sha, H. Lin, J. Hwang, M. Seraydarian, S. L. Craig, C. Tang, *J. Am. Chem. Soc.* **2021**, *143*, 11871–11878.
- [60] Y. Zhang, Z. Wang, T. B. Kouznetsova, Y. Sha, E. Xu, L. Shannahan, M. Ferme-Coker, Y. Lin, C. Tang, S. L. Craig, *Nat. Chem.* **2021**, *13*, 56–62.
- [61] R. Küng, T. Pausch, D. Rasch, R. Göstl, B. M. Schmidt, *Angew. Chem.* **2021**, *133*, 13738–13742; *Angew. Chem. Int. Ed.* **2021**, *60*, 13626–13630.
- [62] a) S. Zarra, D. M. Wood, D. A. Roberts, J. R. Nitschke, *Chem. Soc. Rev.* **2015**, *44*, 419–432; b) M. Yoshizawa, J. K. Klosterman, M. Fujita, *Angew. Chem.* **2009**, *121*, 3470–3490; *Angew. Chem. Int. Ed.* **2009**, *48*, 3418–3438.

Manuscript received: October 26, 2021

Accepted manuscript online: December 8, 2021

Version of record online: January 22, 2022